Bull Eng Geol Environ (2012) 71:569–578
DOI 10.1007/s10064-011-0414-3

ORIGINAL PAPER

Spatial stability of slope cuts in rock massifs using GIS technology and probabilistic analysis

C. Irigaray · R. El Hamdouni · J. D. Jiménez-Perálvarez · P. Fernández · J. Chacón

Received: 30 March 2011 / Accepted: 11 November 2011 / Published online: 17 January 2012

Abstract This paper presents a methodology for the stability analysis of cuts in rock slopes. A kinematic analysis of the different types of failure (planar, wedge, and toppling) is developed using GIS, following which a probabilistic analysis is made of the limit equilibrium in slopes where the conditions for kinematic failure are satisfied. The results were verified by comparing the evaluation against the observed stability conditions in 40 road cuts along 4 km of national road N-340, on the Mediterranean edge of Granada province (southern Spain). The validation analysis showed that for some 90% of the slopes studied there was a reasonable fit between the observed and evaluated stability, indicating the proposed methodology is suitable for the preliminary analysis of the stability conditions on rock slopes.

Keywords Rock slopes · Kinematic analysis · Safety factor · Failure probability · GIS

Résumé Le littoral entre Radès et Ezzahra, au nord-est de la Tunisie, a souffert de l'érosion pendant une forte tempête en 1981. En conséquence, entre 1985 et 1988 un brise-lames a été construit à Radès et deux brise-lames à Ezzahra. L'article présente une étude de l'efficacité de ces structures et considère les autres facteurs qui contrôlent les processus d'accrétion et d'érosion du littoral.

Mots clés Brise-lames · Erosion littorale · Accrétion littorale · Radès-Ezzahra · Tunisie

C. Irigaray (✉) · R. El Hamdouni · J. D. Jiménez-Perálvarez · P. Fernández · J. Chacón
Department of Civil Engineering, ETSICCP, University of Granada, Campus Fuentenueva s/n, Granada 18071, Spain
e-mail: clemente@ugr.es

Introduction

Stability assessments of rock slopes involving civil works are generally preceded by a kinematic analysis which forms the basis for the selection of cut slopes for further assessment of the factor of safety (Hoek and Bray 1981; Norrish and Wyllie 1996). A kinematic analysis is a geometrical method developed using stereographic projections. It can assist in the determination of likely failure modes, the geometrical relationships between discontinuities and the relevant friction angles, and has been reported by several authors (Hoek and Bray 1981; Yoon et al. 2002).

According to the equilibrium-limit method, the failure of a rock mass occurs above a discontinuity when the shear stress surpasses the shear strength of this surface. Generally, this type of analysis is made by the deterministic calculation of the factor of safety (Goodman and Bray 1976; Kumsar et al. 2000; Hoek 2007). However, the uncertainty and/or variability associated with the geotechnical properties of materials hampers the selection of the appropriate values needed for this type of analysis and gave rise to the development of probabilistic methods. Some authors have proposed substituting the use of the standard safety factor, FS, for the reliability index, RI, (e.g Christian et al. 1994) or the probability of failure, PF (Hoek 2007).

Numerous authors have used the equilibrium-limit method for the stability analysis of rock slopes, both from the deterministic standpoint (Sarma 1979; Warburton 1981) as well as the probabilistic approach (Priest and Brown 1983). However, this method has the limitation that the failure mode must be known before it can be applied; that is, the method cannot recognize the failure mode without the help of a prior kinematic analysis (Kim et al. 2004).

The spectacular increase in the availability of computers in recent years and the development of GIS have provided powerful tools to analyse spatial information. GIS has been widely used to analyse stability against slope movements in general (Carrara et al. 1991; Chacón et al. 1996, 2006; Chacón and Corominas 2003; Irigaray et al. 2007), but there are fewer examples of its use in rock slopes (Gokceoglu et al. 2000; Irigaray et al. 2003, 2010; Günther et al. 2004; Kim et al. 2004; Aksoy and Ercanoglu 2007). This paper presents a methodology incorporating ArcGIS 9.3 (ESRI 2009). It was validated by stability analyses for different types of failure controlled by the discontinuities in rock masses at the Mediterranean edge of the province of Granada (southern Spain).

Location of the study area

The study area is located on the coast of Granada (southern Spain) 15–20 km east of the city of Motril (Fig. 1). Geologically, it belongs to the Alpujarride Complex of the Internal Zones of the Betic Cordillera. It is covered by the carbonate materials of the Murtas Unit of Triassic age (Aldaya 1981), although in places the underlying Permo-Triassic phyllites crop out.

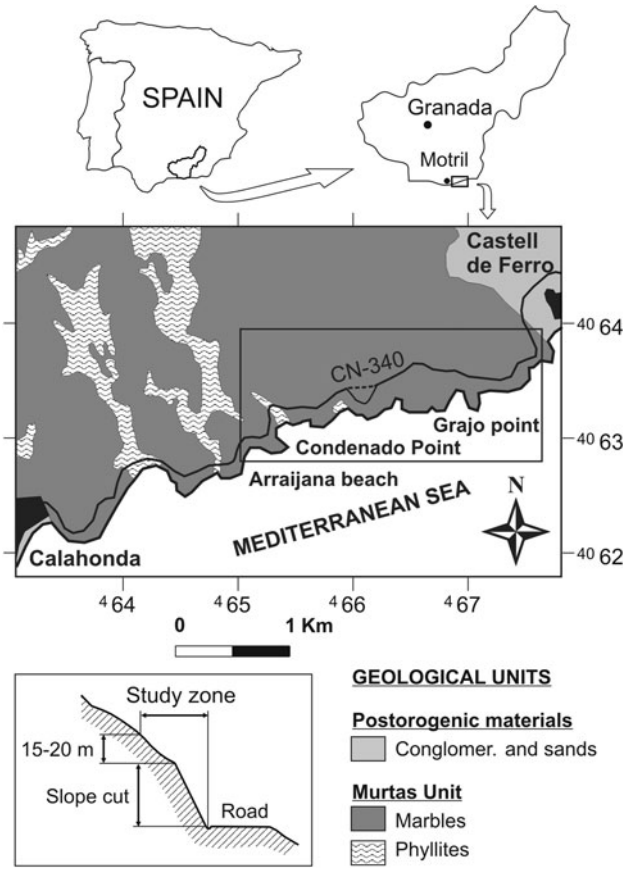

Fig. 1 Location of the study area

Thirteen rock slopes along national highway N-340 (between the Arraijana beach and Castell de Ferro) were selected for study, based on their geological and structural features. The study was limited to the surface area between the highway and a height of between 15 and 20 m above the road. Some of these slopes were sub-divided into sections, either because the ground plan of the slope was curved or because they included significant lithological or structural differences, such that a total of 40 slope units were studied. Figure 2 is an example of one of the studied slope units.

The meteorological records show the maximum temperature in July and August is some 26–27°C while in February the minimum is some 13°C. The mean annual rainfall is 486 mm; the precipitation peaking in March (monthly mean of 69 mm) and December (90 mm) while in July it is as little as 1 mm.

Data collection

Scan line surveys were made of representative slopes, following Hoek and Bray (1981), and Hudson and Priest 1983). A total of 2,330 m of scanline were undertaken for 740 analysed discontinuities and their geomechanical parameters measured, including spacing, resistance to compression, weathering, presence of water, etc. (Irigaray et al. 2003). The tilt test was used to measure the angle of friction (Bruce et al. 1989; Franklin and Dusseault 1989; Barton 2008). Cohesion was not measured but was estimated based on information published on similar rocks (Hoek and Bray 1981; Goodman 1989; Waltham 1999).

Some of the data needed for the analysis were obtained using a Digital Elevation Model (with a 2 × 2 m cell size) and ArcGIS 9.3 (ESRI 2009). The topographic and cartographic information used was prepared by Granada Province Council in 1998 at a scale of 1:2,000.

Table 1 shows the general characteristics and the mean geomechanical parameters for one of the slopes studied. All the information acquired was implemented in the Geographic Information System ArcGIS 9.3 (ESRI 2009).

Methodology and results

Four sets of discontinuities were identified in each of the slope profiles and representative values of the geomechanical properties established. Stereographic projection was used (DIPS 5.0) to identify all the possible intersections between the sets of discontinuities present in each slope.

Fig. 2 Marble slope in the national road N-340 between Calahonda and Castell de Ferro (Granada, Spain)

Table 1 General characteristics and mean geomechanical parameters of the slope T1-a

Mean values of discontinuities (85 measurements):				
Set	1	2	3	4
Dip	68°	53°	33°	37°
Dip direction	273°	233°	137°	332°
Spacing (m)	0.1	0.1	0.3	0.2
Continuity	Sub-continuous	Not continuous	Continuous	Not continuous
Roughness	Slightly rough	Smooth	Slightly rough	Slightly rough
Infilling	No	Clay	Calcite	No
Aperture (mm)	0.1–1	0.1–1	>5	0.1–1
Weathering	Slightly weathered	Slightly weathered	Slightly weathered	Slightly weathered
Groundwater	Dry	Dry	Dry	Dry
Cohesion (kPa)	0	10	50	40
Friction angle (°)	33	32	33	36

Slope unit: T1-a. Excavation method: normal blasting. Maximum altitude: 12.5 m. Length: 110 m. Strike: N330°. Dip: 80°. Shape: rectilinear. Lithology: limestone-dolomitic marbles with alternating clear white and dark ones from centimetres to decimetres in thickness. Age: Triassic. Support measures: None. Breaks visible: formation of several decimetric wedges with low risk of falling. Uniaxial compressive strength: 37 MPa. Unit weight of rock: 26 kN/m^3

The stability conditions in the rock masses were analysed at two different stages (Goodman and Bray 1976; Hoek and Bray 1981; Goodman 1989; Norrish and Wyllie 1996). First, a kinematic analysis was made to determine the likelihood of planar, wedge, and/or toppling failure using GIS ArcGIS 9.3 (ESRI 2009). Where potential failure was identified, the factor of safety (FS) and probability of failure (PF) were determined using ROCPLANE 2.0 and SWEDGE 5.0 (Rocscience 2009b, c).

Kinematic analysis

The kinematic conditions for planar, wedge and toppling failure are recorded along the route corridor (Fig. 3). The slopes that present a greater extension of the zones with geometric instability are T8-c, T-7b, and T-8a, with values >20%. The slopes T-2a, T-7c, T-7d, T-7g, T8-g2, T9-1, T9-2, T11-a, and T13 presented no potential geometric instability (Fig. 3).

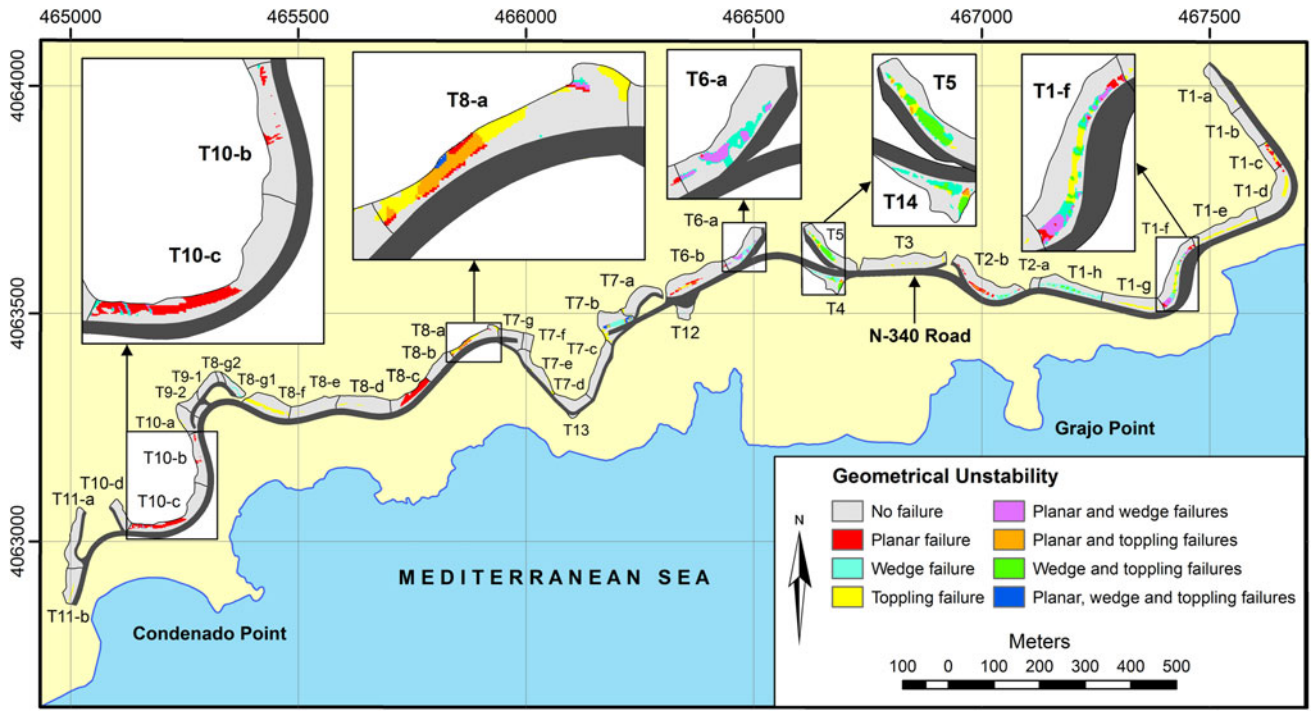

Fig. 3 Map of kinematic conditions for the planar, wedge, and toppling failure

Safety factor and failure probability

Factors of safety were established using limit-equilibrium analysis (Kovári and Fritz 1975; Hoek 2007), based on the parameters given in Tables 2, 3 and 4. In addition, a sensitivity analysis was made in order to determine the influence of the various parameters on the value of the calculated factor of safety. This type of analysis involves the application of the theory of probability to the risk evaluation (Harr 1987; Pine 1992) and provides a medium factor of safety (FS) as well as a probability of failure (PF). The results are given in Table 5.

The results are shown for the calculation of the safety factor by a probabilistic analysis for the cases of planar and wedge failure, made by the programs ROCPLANE 2.0 and SWEDGE 5.0, respectively (Rocscience 2009b, c). The analysis was made in all those slopes where the kinematic analysis indicated pixels that fulfilled the structural conditions of planar or wedge failure.

Planar failure

In the general case, the calculation of safety factor for planar failure of the slope is determined by the following equation (Norrish and Wyllie 1996; Hoek 2007):

$$FS=\frac{cA+\left(W\left(\cos\psi_p-\eta\sin\psi_p\right)-U-V\sin\psi_p+T\cos\theta\right)\tan\phi}{W\left(\sin\psi_p+\eta\cos\psi_p\right)+V\cos\psi_p-T\sin\theta}$$

where FS = factor of safety against sliding along a sheet joint; c = cohesive strength along a sliding surface; A = base area of wedge; W = weight of rock wedge resting on the failure surface; ψ_p = angle of failure surface, measured from horizontal; η = seismic coefficient; U = uplift force due to water pressure on failure surface; V = horizontal force due to water in tension crack (if present); T = force applied by the anchor system (if present); θ = inclination of the anchor, anti-clockwise from normal; ϕ = friction angle of sliding surface.

To determine the input data used for calculating the safety factor for the planar failure by ROCPLANE 2.0 (Rocscience 2009a) the following has been taken into account:

(a) *Geometry and weight* The slopes had no bench and in general had a rather uniform dip, so that the overall slope angle was considered fixed over its entirety. The failure planes were determined from prior kinematic analysis and appear to be almost smooth; thus the waviness angle is considered equal to 0. The overall slope height is considered fixed for the entire extension of the slope based on direct measurement in the field. The slope of the upper face corresponds to the angle of the natural slope from the DEM (Digital Elevation Model), and, given that it can present a certain variability over the slope, it was considered to be a random variable with a normal distribution and a

Table 2 Mean values of the input data used to calculate the probabilistic factor of safety for planar failure

Cut slope ID	Slope			Failure plane		Upper face	Strength	
	Angle (°)	Height (m)	Unit weight (kN/m^3)	No set	Angle (°)	Angle (°)	c (kPa)	ø (°)
T1-a	80	12.5	27	4	37	34	40	36
T1-b	75	12	27	4	43	35	50	30
T1-c	77	15	27	2	43	32	10	30
T1-d	75	15	26	3	61	33	30	34
T1-f	73	26	26	4	44	32	150	35
T1-h	72	29	26	4	62	33	120	34
T2-b	72	20	26	1	62	30	40	32
T4	69	23	26	3	61	34	40	37
T5	65	25	26	1	54	30	10	30
T6-a	67	15	27	4	41	34	40	37
T6-b	70	19	26	4	41	30	60	30
T7-b	68	20	26	4	46	33	5	36
T8-a	65	14	27	4	41	30	5	34
T8-c	62	18	26	4	38	28	5	36
T10-b	68	8	26	3	40	34	150	30
T10-c	46	12	26	4	43	34	20	32

Table 3 Mean values of the input data used to calculate the probabilistic factor of safety for wedge failure

Cut slope ID	Upper face		Slope face		Slope height (m)	Slope length (m)	Unit weight (kN/m^3)
	Dip (°)	DipDir (°)	Dip (°)	DipDir (°)			
T1-a	34	046	80	060	12.5	110	27
T1-b	35	053	75	060	12	95	27
T1-f	32	115	73	125	26	146	26
T1-h	33	200	72	200	29	140	26
T2-b	30	130	72	160	20	90	26
T4	19	285	69	003	16	80	26
T5	30	235	65	225	25	115	26
T6-a	41	115	67	125	15	100	27
T7-b	33	205	68	175	20	75	26
T8-a	30	155	65	155	14	120	27
T8-f	25	217	71	176	17	100	27
T8-g1	35	300	52	310	13	60	27
T10-b	34	62	68	72	8	113	26
T10-c	34	180	46	180	12	85	26
T12	24	189	52	359	6	40	26

standard deviation of 5°. The specific weight of the rock was determined from typical values in the literature (Farmer 1968; Goodman 1989; Waltham 1999). In field observations, no tension cracks were located; however, given the possibility that they could exist and that they were inadvertently overlooked, two situations were considered: without tension cracks and with tension cracks. In the latter, vertical tension cracks were considered with the FS location.

(b) *Water pressure* From field observations, the slopes appeared to be in a dry state (Irigaray et al. 2003). The carbonate nature of the materials (marbles) as well as their structural characteristics indicated drained conditions in all cases hence the water pressure was assumed to be nil.

(c) *External and seismic forces* In the slopes studied, no type of outer reinforcement was used and therefore in this section only seismic force is considered. Based on the Seismic-Resistance Construction Norm of Spain

Table 4 Mean values of the input data of discontinuities used to calculate the probabilistic factor of safety for wedge failure

Cut slope ID	Sets	Joint 1				Joint 2			
		Dip (°)	DipDir (°)	c (kPa)	ϕ (°)	Dip (°)	DipDir (°)	c (kPa)	ϕ (°)
T1-a	1∩4	68	273	0	33	37	332	40	36
T1-b	2∩3	42	125	0	35	73	25	150	29
T1-f	3∩4	68	051	150	34	44	140	150	35
T1-h	1–4	56	259	150	31	62	142	120	34
T2-b	1–4	62	223	40	32	52	115	20	35
T4	2–3	80	280	15	37	61	062	40	37
T5	1–4	54	277	10	30	73	146	5	35
T6-a	3–4	70	68	50	36	41	150	40	37
T7-b	3–4	74	056	150	36	46	138	5	36
T8-a	1–4	85	026	5	34	41	126	5	34
T8-f	1–4	75	025	10	36	38	117	30	36
T8-g1	1–2	88	244	10	35	58	286	50	36
T10-b	2–3	62	351	10	32	54	051	150	30
T10-c	1–4	63	276	70	34	43	172	20	32
T12	3–4	77	258	150	31	47	298	10	32

Table 5 Mean factor of safety (FS) and probability of failure (PF) obtained into the ROCPLANE and SWEDGE analysis

Cut slope ID	ROCPLANE analysis				SWEDGE analysis	
	Without tension crack		With tension crack			
	FS	PF (%)	FS	PF (%)	FS	PF (%)
T1-a	1.23	7	1.01	45	5.91	0
T1-b	1.44	1	1.46	10	4.94	0
T1-c	0.59	100	0.55	100	–	–
T1-d	0.92	63	0.79	87	–	–
T1-f	1.67	0	1.31	0	2.63	0
T1-h	2.10	0	1.83	0	2.76	0
T2-b	1.13	29	1.00	50	1.21	9
T4	1.25	18	1.14	30	2.68	0
T5	0.48	100	0.46	100	1.22	6
T6-a	1.17	27	0.98	53	1.88	0
T6-b	1.24	15	1.01	48	–	–
T7-b	0.60	100	0.58	100	0.70	100
T8-a	0.68	100	0.65	100	0.72	100
T8-c	0.78	100	0.76	100	–	–
T8-f	–	–	–	–	5.33	0
T8-g1	–	–	–	–	3.88	0
T10-b	4.36	0	3.03	0	17.28	0
T10-c	2.78	4	2.61	4	3.55	0
T12	–	–	–	–	19.01	0

NCSR-02 (Ministerio de Fomento 2002), the seismic coefficient of the study sector (town of Gualchos) is equal to 0.13 g.

(d) *Shear strength* The relationship between the shear strength (τ) of the failure plane and the normal stress (σ_n) acting on the plane is represented by the Mohr–Coulomb equation:

$$\tau = c + \sigma_n \tan \phi$$

where ϕ is the friction angle of the failure plane and c is the cohesion.

The friction angle of the discontinuities has been estimated from data measured directly in the field by the tilt test (Barton 1981; Franklin and Dusseault 1989). From

these results, and taking into account the data from the literature (Farmer 1968; Hoek and Bray 1981; Goodman 1989; Waltham 1999) a normal distribution was considered for this variable, with a standard deviation of 5°. No experimental data were available to determine the cohesion of the discontinuities for the study zone hence this parameter was estimated on the basis of information published for similar rocks (Farmer 1968; Hoek and Bray 1981; Goodman 1989; Waltham 1999). A normal truncated distribution was assumed with a minimum value of 0 kPa, a maximum equal to double the mean values, and a standard deviation of 10 kPa.

(e) S*ampling technique* The sampling technique used in the probabilistic analysis was the Latin Hypercube (Iman et al. 1980), which provides results comparable to those of the Monte Carlo technique (Harr 1987) but with fewer samples (Hoek 2007).

Table 2 shows the mean values of the input data used to calculate the probabilistic factor of safety for planar failure.

Wedge failure

In the case of wedge failure, the calculation of the safety factor is given below[1] (Kumsar et al. 2000): where FS = factor of safety; W = weight of the rock wedge resting on failure surfaces; i_a = intersection angle; η = seismic coefficient; β = inclination angle of a dynamic force ($\beta = 0$ for seismic forces); c = cohesive strength along the sliding surfaces; U_s = water force acting on the face of the slope (if present); U_t = water force acting on the upper part of the slope (if present); U_b = force caused by fluid pressure normal to each joint; A_1 and A_2 = joint surface areas; ϕ = friction angle; λ = wedge factor by Kovári and Fritz (1975):

$$\lambda = \frac{\cos\omega_1 + \cos\omega_2}{\sin(\omega_1 + \omega_2)}$$

where ω_1 and ω_2 are the angles between the surfaces of each joint with the vertical.

Taking into account the same considerations as in the analysis of the planar failure, in the probabilistic analysis for wedge failure neither benches, tension cracks, nor water pressure were considered. The Latin HyperCube sampling method was used.

Tables 3 and 4 show the mean values of these data for the talus that fulfil the kinematic conditions of wedge failure.

[1]

$$FS = \frac{[\lambda[W(\cos i_a - \eta\sin(i_a+\beta)) + U_s\sin i_a + U_t\cos i_a] - U_b]\tan\phi + c(A_1+A_2)}{W(\sin i_a + \eta\cos(i_a+\beta) - U_s\cos i_a + U_t\sin i_a}$$

Table 5 shows the FS and PF calculated for the different conditions studied in the slopes where the kinematic conditions were satisfied. The results show that

(a) The slopes that presented the greatest probability of failure, both for planar failure and wedge failure (FS < 1 and PF = 100%) were slopes T7-b and T8-a.
(b) Slopes T1-c and T8-c also presented the greatest probability of failure, but, in these, planar failure was geometrically possible.
(c) Slope T5 presented the maximum probability of planar failure, and a lower probability of wedge failure (FS = 1.22 and PF = 6%). However, the extension where the planar failure was geometrically possible was very reduced in this slope.
(d) Slopes T1-d, T2-b, T4, T6-b, T8-f, and T10-c could also present instability problems but with low probabilities of failure (maximum 63% in T1-d).
(e) The rest of the slopes presented very low or null probabilities of failure.

Validation of the results

With the aim of testing the validity of the results, a comparative analysis was made between the evaluation and field observation.

Table 6 shows the failures detected in the field, as well as the overall evaluation of the stability of the slopes studied. It also includes the results of the kinematic and equilibrium limit analyses.

Table 7 shows the failure categories for the 40 slopes. It can be seen that the mathematical analyses for 36 of the 40 slopes studied (90%) were generally consistent with the stability observed in the field. The five slopes directly observed as "unstable" were compatible with failure, both from the geometric and limit equilibrium analysis. In the ten slopes showing "stable" conditions, it was confirmed that failure kinematic or limit equilibrium conditions were not accomplished. The seven slopes directly observed as "rather unstable" included five slopes fulfilling all the failure requirements, one slope which showed the kinematic conditions for toppling failure and only one slope which did not satisfy geometric failure conditions. In the 18 slopes directly observed as "rather stable", only three of them were considered as failed using the proposed methodology while the remaining 15 slopes show various different stable conditions (Table 7).

Determination of the appropriate slopes for the talus

Prior to the design of an engineering work in a rock mass, it is important to determine a stable slope angle which is cost effective. To determine whether the slopes studied were

Table 6 Failures detected and overall evaluation of the stability of all the slopes studied

Cut slope ID	KF			PF (%)		Observed failures	Observed stability
	P	W	T	P	W		
T1-a	Y	Y	Y	7–45	0	Plane failure, falling blocks	Rather stable
T1-b	Y	Y	N	1–10	0	Plane failure, few wedge failures	Rather stable
T1-c	Y	N	Y	100	–	Plane failure, falling blocks	Rather unstable
T1-d	Y	N	Y	87	–	Falling blocks	Rather unstable
T1-e	N	N	Y	–	–	Small falling blocks	Rather stable
T1-f	Y	Y	Y	0	0	Small falling blocks	Rather stable
T1-g	N	N	Y	–	–	Small falling blocks	Rather stable
T1-h	Y	Y	Y	0	0	Small wedge failure	Rather stable
T2-a	N	N	N	–	–	No	Stable
T2-b	Y	Y	Y	29–50	9	Plane and wedge failures	Unstable
T3	N	N	Y	–	–	Small falling blocks	Rather stable
T4	Y	Y	Y	18–30	0	Plane failure, falling blocks	Rather unstable
T5	Y	Y	Y	100	6	Falling blocks, wedge failure	Unstable
T6-a	Y	Y	N	27–53	0	Plane failure	Rather unstable
T6-b	Y	N	Y	15–48	–	Plane failure	Rather unstable
T7-a	N	N	Y	–	–	Small blocks	Rather Stable
T7-b	Y	Y	Y	100	100	Large wedge failure	Unstable
T7-c	N	N	N	–	–	No	Stable
T7-d	N	N	N	–	–	No	Stable
T7-e	N	N	Y	–	–	Small falling blocks	Rather stable
T7-f	N	N	N	–	–	Falling blocks	Rather unstable
T7-g	N	N	N	–	–	No	Rather stable
T8-a	Y	Y	Y	100	100	Plane failure, falling blocks, wedge failure	Unstable
T8-b	N	N	N	–	–	No	Rather stable
T8-c	Y	N	N	100	–	Plane failure, falling blocks	Unstable
T8-d	N	N	Y	–	–	Falling blocks	Rather unstable
T8-e	N	N	Y	–	–	Falling blocks	Rather stable
T8-f	N	Y	Y	–	0	Falling blocks, wedge failure	Rather stable
T8-g1	N	Y	N	–	0	Small wedge failure	Rather stable
T8-g2	N	N	N	–	–	No	Stable
T9-1	N	N	N	–	–	No	Stable
T9-2	N	N	N	–	–	No	Stable
T10-a	N	N	Y	–	–	Small falling blocks	Rather stable
T10-b	Y	Y	N	0	0	Small falling blocks	Rather stable
T10-c	Y	Y	N	4	0	Small plane failure	Rather stable
T10-d	N	N	Y	–	–	No	Stable
T11-a	N	N	N	–	–	No	Stable
T11-b	N	N	Y	–	–	Small falling blocks	Rather stable
T12	N	Y	N	–	0	No	Stable
T13	N	N	N	–	–	No	Stable

KF Kinematic failure; *P* Planar failure; *W* Wedge failure; *T* Toppling failure; *Y* Yes; *N* No; *PF* Probability of failure

sufficiently stable, determinations were made of the slope angle which would give an FS against planar and wedge failure, of >1.5, assuming the remainder of the parameters considered in the equilibrium-limit analysis remained unchanged. Table 8 shows the recommended angles, which in some cases indicate a reduction in angle of some 20°. Where the recommended angles could not be achieved, whether for geometric or economic reasons, it is highly

Table 7 Distribution of the number of slopes that fulfil different conditions for failure and observed stability

Observed stability	Plane or wedge failure		Toppling failure	No kinematic conditions for failure
	LE	NLE		
Unstable (5)	5	0	0	0
Rather unstable (7)	5	0	1	1
Rather stable (18)	3	5	8	2
Stable (10)	0	1	1	8

LE Compatibility with failure according to the limit equilibrium analysis. No compatibility with failure according to the limit equilibrium analysis

Table 8 Actual slope angle (A) and recommended slope angle (α) for unstable slopes to reach a safety factor higher than 1.5

Cut slope ID	T1-c	T1-d	T2-b	T4	T5	T6-a	T6-b	T7-b	T8-a	T8-c
A (°)	77	75	72	69	65	67	70	68	65	62
α (°)	45	67	58	66	46	55	55	47	42	39

recommended that an adequate support of some outer reinforcement be applied (wire mesh, anchors, etc.).

Discussion and conclusions

The aim of the present work was to propose a methodology for analysing the stability conditions of rock slopes. It involves two stages:

1. A kinematic analysis of the different types of failure (planar, wedge, and toppling) using GIS.
2. A probabilistic analysis of the limit equilibrium in the slopes where the conditions of kinematic failure were satisfied.

The results were verified by the comparing the instability evaluation and the instability conditions observed on site.

In the case of the study area, situated on the national highway N-340 in southern Spain, the kinematic analysis indicated that 27 of the 40 slopes studied presented geometric conditions consistent with failure. Of these 27 slopes, 7 had safety factors lower than 1 for planar or toppling failure, of which 5 presented a probability of failure of 100% with the parameters estimated. The validation analysis showed that, overall, for 90% of the slopes studied there was a reasonable fit between the calculated and observed stability, indicating the methodology is useful for a preliminary analysis.

The main limitation of this type of analysis is the estimation of the parameters of the discontinuities, especially the friction and cohesion angle, particularly taking into account local conditions, as well as the climate and geomorphology. The results for the basic friction angles determined from tilt tests were corrected taking into account published experimental results on peak friction angle. More limitations were found in the selection of cohesion values, as it was not possible to make direct measurements between discontinuity planes.

The methodology proposed should be used in combination with other sources of information and analysis methods, and only in the preliminary phases of the design and planning of engineering works. However, in these preliminary phases, GIS constitutes a quick, inexpensive and effective tool for analysing the spatial stability of natural and cut slopes, which can provide useful information when time and economic resources are limited and indicate areas where more specific investigations and analyses should be focussed.

Acknowledgments This research was supported by projects CGL2008-04854 funded by the Ministry of Science and Education of Spain, and Excellence Project P06-RNM-02125, funded by the Regional Government. Rainfall dates have been supplied by the National Meteorological Institute of Spain. It was developed in the RNM-121 Research Group funded by the Andalusian Research Plan.

References

Aksoy H, Ercanoglu M (2007) Fuzzified kinematic analysis of discontinuity-controlled rock slope instabilities. Eng Geol 89:206–219

Aldaya F (1981) Mapa geológico de España, E. 1:50.000, 1056 (Albuñol). IGME, Madrid

Barton N (1981) Shear strength investigation for surface mining. In: 3rd International Conference on stability surface mining, Vancouver

Barton N (2008) Shear strength of rockfill, interfaces and rock joints, and their points of contact in rock dump design. In: Fourie A (ed) Rock dumps. Australian Centre for Geomechanics, Perth

Bruce IG, Cruden DM, Eaton TM (1989) Use of a tilting table to determine the basic friction angle of hard rock samples. Can Geotech J 26(3):474–479

Carrara A, Cardinali M, Detti R, Guzzetti F, Pasqui V, Reichenbach P (1991) GIS techniques and statistical models in evaluating landslide hazard. Earth Surf Proc Land 16:427–445

Chacón J, Corominas J (2003) Special issue on landslides and GIS. Nat Hazards 30(3):263–512

Chacón J, Irigaray C, El Hamdouni R, Fernández T (1996) From the inventory to the risk analysis: improvements to a large scale G.I.S. method. In: Chacón J, Irigaray C, Fernández T (eds) Landslides. Balkema, Rotterdam, pp 335–342

Chacón J, Irigaray C, Fernández T, El Hamdouni R (2006) Engineering geology maps: landslides and geographical information systems. Bull Eng Geol Environ 65:341–411

Christian JT, Ladd CC, Baecher GB (1994) Reliability applied to slope stability analysis. J Geotech Eng ASCE 120:2180–2207

ESRI (2009) ArcGIS Desktop 9.3. Environmental Systems Research Institute, Inc (ESRI) http://www.esri.com/

Farmer IW (1968) Engineering properties of rocks. Spon Ltd, London

Franklin JA, Dusseault MB (1989) Rock engineering. McGraw-Hill, New York

Gokceoglu C, Sonmez H, Ercanoglu M (2000) Discontinuity controlled probabilistic slope failure risk maps of the Altindag (settlement) region in Turkey. Eng Geol 55(4):277–296

Goodman RE (1989) Introduction to rock mechanics. Wiley, New York

Goodman RE, Bray JW (1976) Toppling of rock slopes. In: Proceedings of the specialty conference on rock engineering for foundations and slopes. American Society of Civil Engineers (ASCE), New York, pp 201–223

Günther A, Carstensen A, Pohl W (2004) Automated sliding susceptibility mapping of rock slopes. Nat Hazards Earth Syst Sci 4(1):95–102

Harr ME (1987) Reliability-based design in civil engineering. McGraw-Hill, New York

Hoek E (2007) Practical rock engineering. Rocscience-Hoek's Corner, USA http://www.rocscience.com/education/hoeks_corner

Hoek E, Bray JW (1981) Rock slope engineering. Institution of Mining and Metallurgy, London

Hudson JA, Priest SD (1983) Discontinuity frequency in rock masses. Int J Rock Mech Mining Sci Geomech Abst 20(2):73–89

Iman RL, Davenport JM, Zeigler DK (1980) Latin Hypercube sampling (a progam user's guide). Technical Report SAND 79-1473. Sandia Laboratories, Albuquerque

Irigaray C, Fernández T, Chacón J (2003) Preliminary rock-slope-susceptibility assessment using GIS and the SMR classification. Nat Hazards 30:309–324

Irigaray C, Fernández T, El Hamdouni R, Chacón J (2007) Evaluation and validation of landslide-susceptibility maps obtained by a GIS matrix method: examples from the Betic Cordillera (southern Spain). Nat Hazards 41:61–79

Irigaray C, El Hamdouni R, Jiménez-Perálvarez JD, Fernández P, Chacón J (2010) GIS application to a kinematics analysis and slope stability assessment of slope cuts on rock massifs along a national road in Southern Spain. In: Williams et al (eds) Geologically Active. Taylor and Francis Group, London, pp 1949–1957

Kim KS, Park HJ, Lee S, Woo I (2004) Geographic information system (GIS) based stability analysis of rock cut slope. Geosci J 8(4):391–400

Kovári K, Fritz P (1975) Stability analysis of rock slopes for plane and wedge failure with the aid of a programmable pocket calculator. In: 16th symposium Rock merchandise. ASCE, Minneapolis

Kumsar H, Aydan Ö, Ulusay R (2000) Dynamic and static stability assessment of rock slopes against wedge failures. Rock Mech Rock Eng 33:31–51

Ministerio de Fomento (2002) Real Decreto 997/2002, de 27 de septiembre, por el que se aprueba la norma de construcción sismorresistente: parte general y edificación (NCSR-02). BOE, n° 24, de 11 de octubre de 2002, pp 35898–35967

Norrish NI, Wyllie DC (1996) Rock slope stability analisys. In: Turner AK, Schuster RL (eds) Landslides, investigation and mitigation. National Research Council, Washington, pp 391–425

Pine RJ (1992) Risk analysis design applications in mining geomechanics. Trans Inst Min Metall 101:149–158

Priest SD, Brown ET (1983) Probabilistic stability analysis of variable rock slopes. Trans Inst Min Metall 92:1–12

Rocscience (2009a) Dips 5.0 graphical & statistical analysis of orientation data. © 2009 Rocscience Inc http://www.rocscience.com/

Rocscience (2009b) RocPlane 2.0 Planar sliding stability analysis for rock slopes. © 2009 Rocscience Inc http://www.rocscience.com/

Rocscience (2009c) Swedge 5.0 Surface Wedge Stability Software. © 2009 Rocscience Inc http://www.rocscience.com/

Sarma SK (1979) Stability analysis of embankments and slopes. J Geotech Eng ASCE 105:1511–1524

Waltham AC (1999) Foundations of engineering geology. E and FN Spon, London

Warburton PM (1981) Vector stability analysis of an arbitrary polyhedral rock block with any number of free faces. Int J Rock Mech Min 18(5):415–427

Yoon WS, Jeong UJ, Kim JH (2002) Kinematic analysis for sliding failure of multi-faced rock slopes. Eng Geol 67:51–61